CRYSTAL STRUCTURE DETERMINATION, AND DFT CALCULATIONS OF DICHLOROBIS(DIMETHYLSULFOXIDE-O)COPPER(II)

H. Chebbi[1,2], M. Chebbi[3], A. Guesmi[2], Y. Arfaoui[3]

[1]*Preparatory Institute in the Studies of Engineers of Monastir, University of Monastir, Tunisia*
 E-mail: chebhamouda@yahoo.fr
[2]*Laboratory of Materials and Crystallochemistry, Department of Chemistry, Faculty of Science, University of Tunis El Manar, Tunisia*
[3]*Laboratory of Physical Chemistry of Condensed Materials, Department of Chemistry, Faculty of Science, University of Tunis El Manar, 2092, Tunisia*

The crystal structure of dichlorobis(dimethylsulfoxide-O)copper(II), $[CuCl_2(DMSO)_2]$ (**I**), previously determined by Willett and Chang, is reinvestigated. It crystallizes in the orthorhombic system with the space group *Pnma* (N°62), $Z = 4$, and unit cell parameters $a = 8.053(1)$ Å, $b = 11.642(5)$ Å, $c = 11.347(3)$ Å. Our structure determination is of a significantly higher precision in terms of bond lengths, angles, and *R* factors (e.g., Cu1—O1 = 1.9737(24) Å, O1—Cu1—O1^i = 173.08(13)° (symmetry code: ^{i} *x*, 1/2–*y*, *z*) and $R(F^2) = 0.046$ compared to 1.955(4) Å, 173.0(3)° and $R(F) = 0.075$). In contrast to the previous investigation, all H atoms are placed at calculated positions. In the title molecule, the Cu^{II} atom is five coordinated in a distorted square pyramidal geometry. Thus, as reported previously, it can be shown that the crystal structure consists of $[CuCl_2(DMSO)_2]$ molecules which, by virtue of long Cu—Cl interactions, are tied together to form chains parallel to the [100] direction. The density functional theory (DFT) optimized structure at the B3LYP/6-311++G(2*d*,2*p*) level is compared with the experimentally determined molecular structure. The HOMO—LUMO energy gap and other related molecular properties are also calculated. Comprehensive experimental and theoretical structural studies on the studied complex are carried out by FT-IR and UV-visible spectroscopies.

INTRODUCTION

Many complexes of dimethylsulphoxide, $(CH_3)_2SO$ (hereafter abbreviated DMSO), with transition metals have previously been reported [1—5]. The studied compound, $[CuCl_2(DMSO)_2]$ (**I**), is an example of this class of materials. Its structure determination was undertaken within a project on the preparation and structural investigation of new coordination compounds based on copper(II) halides and organic bases. Our results are of a significantly higher precision in terms of bond lengths, angles, and *R* factors. Moreover, with the aid of literature, it is clear that there is no quantum mechanical study on the title complex which has motivated us to perform a detailed quantum mechanical analysis in order to understand the vibrational modes and HOMO—LUMO properties. The present paper reports a determination of the crystal structure of dichlorobis(dimethylsulfoxide-O)copper(II), with greater precision and accuracy. The geometrical parameters obtained from X-ray diffraction (XRD) studies are

compared with the calculated (DFT) values using the 6-311++G($2d,2p$) basis set. Therefore, in the present study, it is planned to have a combined experimental and theoretical investigation of FT-IR and UV-visible spectroscopies. The HOMO—LUMO energy gap and other related molecular properties were also calculated.

<div align="center">EXPERIMENTAL AND COMPUTATIONAL METHODS</div>

Synthesis and crystallization. The title compound was taken in an attempt to prepare new coordination compounds based on copper(II) halides and organic bases, in a 1:2 water:DMSO solution. The reaction mixture solution was stirred for 30 min and allowed to stand for a week at room temperature. Light green needle-like single crystals, suitable for the X-ray analysis, were grown by slow evaporation. The homogeneity was checked by powder X-ray diffraction.

FT-IR and UV-visible analysis. The FT-FIR spectrum of the title compound was recorded in a KBr pellet in the range 4000—400 cm^{-1} with a Perkin-Elmer spectrophotometer. The ultraviolet absorption spectrum of **I** was examined in the range 200—800 nm using a Cary 500 UV-VIS-NIR spectrometer. The UV pattern is taken from a 10^{-4} molar solution of **I** dissolved in ethanol as a solvent. The FTIR and UV-Vis spectral measurements were carried out at the Department of Chemistry, Faculty of Science, University of Tunis El Manar.

Single crystal X-ray crystallography. The X-ray diffraction analysis of complex **I** was performed on an automated four-circle Enraf-Nonius CAD-4 diffractometer with a graphite monochromated MoK_α radiation source ($\lambda = 0.71073$ Å).

The crystallographic data of **I**: $C_4H_{12}Cl_2CuO_2S_2$, $FW = 290.70$, $T = 293$ K, crystal size 0.22×0.17× ×0.12 mm, orthorhombic, *Pmna*, $a = 10.053(1)$ Å, $b = 11.642(5)$ Å, $c = 11.347(3)$ Å, $V = 1063.8(6)$ Å^3, $Z = 4$, $\rho_{calc} = 1.817$ g/cm^3, $\mu(MoK_\alpha) = 2.906$ mm^{-1}, a total of 3330 reflections ($\theta_{min/max} = 2.5/27°$), 1157 observed reflections ($I \geq 2\sigma(I)$), 58 parameters. GOOF = 1.183, $R_1 = 0.045$, $wR_2 = 0.126$ ($I \geq 2\sigma(I)$), $wR_2 = 0.127$ (all data), max / min diff. peak 0.72 / –1.34 e/Å^3.

The reflections were corrected for Lorentz and polarization effects followed by the psi-scan absorption correction [6]. The data reduction were processed with XCAD4 [7] included in the WINGX software package [8]. The structure was solved by direct methods using SHLEXS-97 [9] and the refinement was made against F^2 using SHLXL-97 [9]. All non-hydrogen atoms were refined with anisotropic atomic displacement parameters. All H atoms were placed at calculated positions and treated using a riding model, fixing the C—H distances of 0.96 Å and $U_{iso}(H) = 1.5U_{eq}(C)$. The final Fourier maps showed no peaks of chemical significance. The structure representation was prepared using Diamond [10]. The WinGX software was used to prepare the material for publication. CIF file containing complete information about the structure of **I** was deposited with the Cambridge Crystallographic Data Center (No. 1055517); the file is freely available upon request from the following web site: http://www.ccdc.cam.ac.uk/data_request/cif.

Computational details. The DFT method developed by Hohenberg and Kohn has been proved to be a good tool for the theoretical rationalization of structural and electronic properties of atoms, molecules, and solids [11, 12]. Thus, in this study, Becke′s three-parameter hybrid exchange functional with the Lee—Yang—Parr (B3LYP) correlation functional [13, 14] and the 6-311++G($2d,2p$) basis set [15] implemented in the Gaussian 09 program [16] were used in all calculations. The Gauss View program [17] was used for visualization of the structure and simulation of the vibrational spectra. The DFT structure optimization of the title compound was performed, starting from the X-ray geometry. Harmonic vibrational frequencies were also computed using the same functional and basis set. An empirical uniform scaling factor of 0.983 up to 1700 cm^{-1} and 0.958 for greater than 1700 cm^{-1} [18] have been used to counterbalance the systematic difference caused by basis set incompleteness, neglect of electron correlation and vibrational anharmonicity [19]. The UV spectrum was computed with the TD-DFT approach and the CPCM quantum model solvation in ethanol. Some electronic properties were also calculated, as well as the graphical representations of HOMO and LUMO.
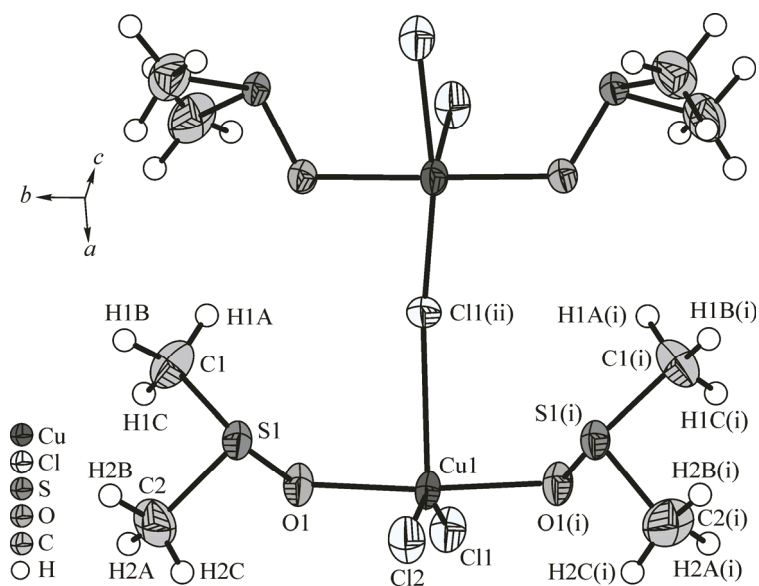
Fig. 1. Molecular structure of **I**, with the atom numbering scheme.
Displacement ellipsoids are drawn at the 50 % probability level.
Symmetry codes: (i) $x,1/2-y, z$; (ii) $1/2+x, 1/2-y, 1/2-z$

RESULTS AND DISCUSSION

X-ray crystallography. In the title complex the crystallographically unique Cu atom is coordinated by two chlorine atoms (av. d(Cu—Cl) = 2.2866(10) Å) and two oxygen atoms from two symmetric DMSO molecules (d(Cu—O) = 1.973(2) Å). The fifth ligand is an additional chlorine atom (d(Cu—Cl) = 2.6984(9) Å). The examination of these bond distances indicate that it is appropriate to describe the geometry as distorted square pyramidal rather than distorted trigonal bipyramidal (Fig. 1). The bond valence sum (BVS) calculations [20] for Cu gives a value of +1.78 indicating an oxidation state of +II.

The crystal structure of the title compound consists of $CuCl_2(DMSO)_2$ moieties tied together by long Cu—Cl interactions to form infinite chains parallel to the short crystallographic a axis (Fig. 2). The copper and chlorine atoms in **I** are in special positions at the mirror planes, $y = 1/4$ and $y = 3/4$.
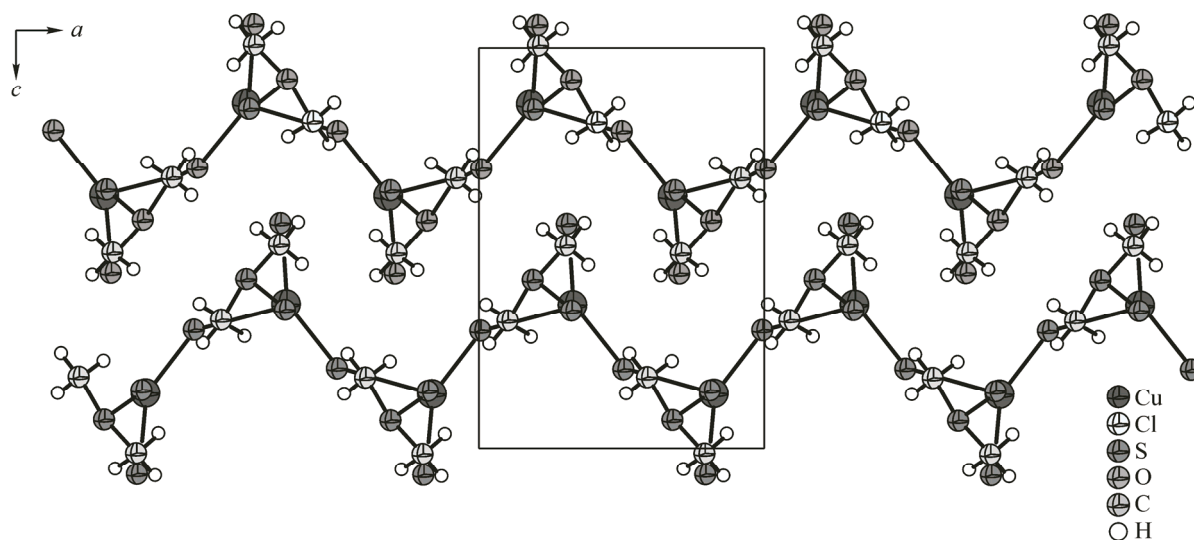

Fig. 2. Fragment of the crystal packing viewed in the *ac* plane

T a b l e 1

Comparison of selected geometric data of **I** (Å, deg.) *from the* X-ray *experiment and the* DFT *calculation*

Selected bond	X-ray	DFT (B3LYP)	Selected bond	X-ray	DFT (B3LYP)	Selected angle	X-ray	DFT (B3LYP)
Cu1—O1	1.973(2)	2.015	C1—H1A	0.960	1.088	O1—Cu1—O1	173.08(13)	155.7
Cu1—Cl1	2.290(1)	2.292	C1—H1B	0.960	1.086	O1—S1—C1	104.05(15)	100.9
Cu1—Cl2	2.280(1)	2.219	C1—H1C	0.960	1.087	O1—S1—C2	104.69(15)	105.5
S1—O1	1.538(2)	1.544	C2—H2A	0.960	1.086	C1—S1—C2	99.7(2)	98.4
S1—C1	1.770(3)	1.816	C2—H2B	0.960	1.088	S1—O1—Cu1	118.11(11)	124.4
S1—C2	1.777(4)	1.815	C2—H1C	0.960	1.087	S1—C1—H1A	109.5	111

DFT studies. Structural analysis: DFT with the Gaussian 09 program package employing the B3LYP (three parameter Becke—Lee—Yang—Parr) method with the 6-311++G(2d,2p) basis set is used to determine optimized bond lengths and angles. The comparison of the experimental data with those obtained by the theoretical study reveals that all optimized bond lengths and bond angles are slightly larger than the experimental values (Table 1). The observed discrepancies between the theoretical and experimental results may be attributed to different environments of the molecule, being the isolated state in the gas phase for the theoretical study, whereas the experimental values are for the molecule in the solid state, thereby subjected to intermolecular forces.

FT-IR spectral analysis. To gain a better understanding of the properties of [CuCl$_2$(DMSO)$_2$], we further explored the stability of this compound in the gas state, having calculated the harmonic frequencies and compared the results with those observed fundamental vibrational frequencies. The calculated wavenumbers are usually higher than the corresponding experimental values. The major reason is that the experimental values are anharmonic frequencies while the calculated values are harmonic frequencies [19]. To avoid this systematic difference, the calculated wavenumbers are usually scaled by one scaling factor. The scaling factors are taken as 0.983 for frequencies less than 1700 cm^{-1} and 0.958 for frequencies above 1700 cm^{-1} for the B3LYP/6-311++G(2d,2p) level [18] in the Gaussian program calculations. The spectrum shows several well defined bands: the intense band in the IR spectrum at 924 cm^{-1} can be assigned to ν_{sym}(S = O) which is also observed in the calculated spectrum at 930 cm^{-1}. According to the literature data [21—23], the bands observed at 2972 cm^{-1} and 2858 cm^{-1} were assigned to ν_{asym}(C—H) and ν_{sym}(C—H) respectively. The theoretical counterparts of these bands are noticed at 2990 cm^{-1} and 2865 cm^{-1}. The main observed and calculated bands with their assignments are shown in Table 2. The comparison of the observed fundamental frequencies of (**I**) and the IR spectrum calculated by DFT (B3LYP) show good agreement between the frequencies (Fig. 3).

UV-Vis spectral analysis. The UV-Vis electronic absorption spectra of (**I**) in the ethanol solvent was recorded within the range 200—800 nm. The electronic absorption maxima are observed at 309 nm and above 800 nm. These values are similar to those found in [PdCl$_2$(DTO)] and [NidCl$_2$(DTO)] compounds (309 nm, 781 nm and 315 nm, 665 nm) [24]. The band observed at

T a b l e 2

Comparison of the experimental and calculated frequencies with the proposed assignments of **I**

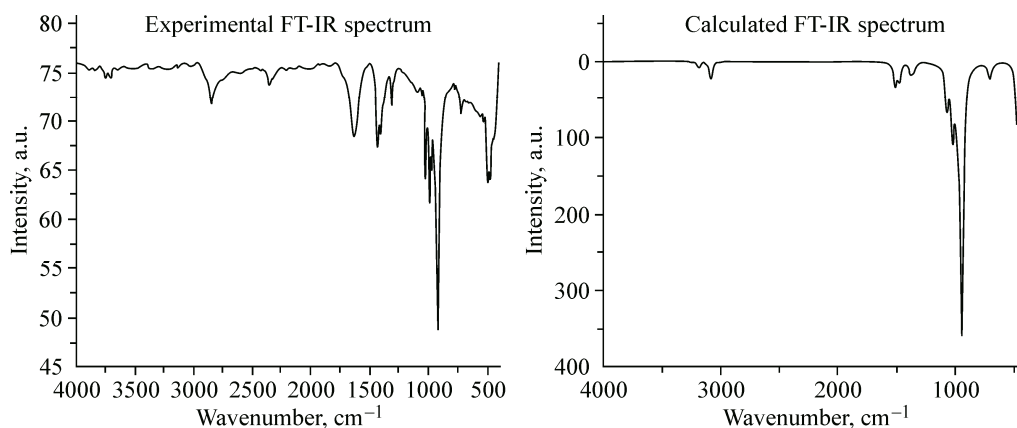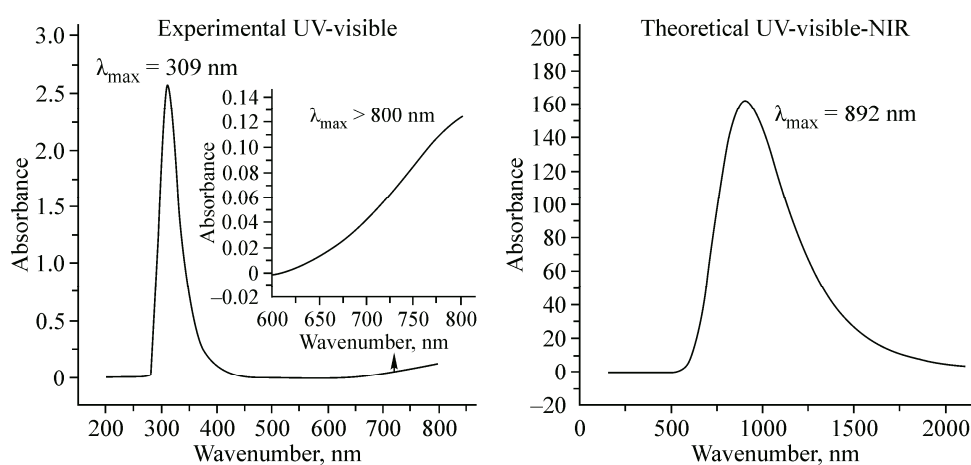| IR experimental frequency, cm^{-1}	Calculated frequency, cm^{-1}	Assignment	IR experimental frequency, cm^{-1}	Calculated frequency, cm^{-1}	Assignment
495	447	δ(CH$_3$)+δ(S=O)	1033	1043	
699	683	δ(CH$_3$) out of plane	1319	1348	δ(CH$_3$) umbrella effect
924	930	ν_{sym}(S=O)	2858	2865	ν_{sym}(C—H)
986	999	δ(CH$_3$) in plane	2972	2990	ν_{asym}(C—H)

Fig. 3. Observed and calculated FT-IR spectra of **I**

Fig. 4. Experimental UV-visible (ethanol) and theoretical UV-visible-NIR spectra

309 nm was ascribed to the n—π^* transition of the —S = O group, however the second band at λ_{max} above 800 nm can be attributed to the d—d transition. Transition metal complexes usually show three types of electronic bands covering a wide range: d—d (crystal-field) transitions (300—1500 nm), charge-transfer transitions (200—500 nm), and transitions localized on the ligands. The last are $n \to \pi^*$ or $\pi \to \pi^*$ and regularly occur in the UV region affected by the type of coordination [24]. In order to estimate excitation energies and oscillator strengths of compounds in the ethanol solvent, TD-DFT calculations were performed using the DFT method at the B3LYP/6-311G++($2d,2p$) level. Major contributions to the electronic transitions were specified with the aid of the Gaussian program [16]. As shown in Fig. 4, the band found at 309 nm is due to HOMO—LUMO transitions while the bands at λ_{max} above 800 nm (892 nm (cal.)) are assigned to Cu(d)—Cu(d) transitions. Experimental and calculated UV-Vis spectra of the title compound are shown in Fig. 4 and it is seen that the calculated UV-Vis-NIR spectra of **I** are complementary to the experimental UV—Vis spectra.

Frontier molecular orbital analysis. The most important frontier molecular orbitals (FMOs) such a HOMO and LUMO play a crucial part in the chemical stability of the molecule [24]. The HOMO represents the ability to donate an electron and the LUMO represents the ability to accept an electron. The energy gap between HOMO and LUMO also determines the chemical reactivity, optical polarizability, chemical hardness and explains the charge transfer interaction that takes place within the molecule [25]. A molecule with a small FMO gap is more polarizable and is generally associated with a high chemical reactivity; a low kinetic stability is also termed as a soft molecule [26]. The plots of HOMO and LUMO were calculated using B3LYP/6-311++G($2d,2p$) and are shown in Fig. 5.
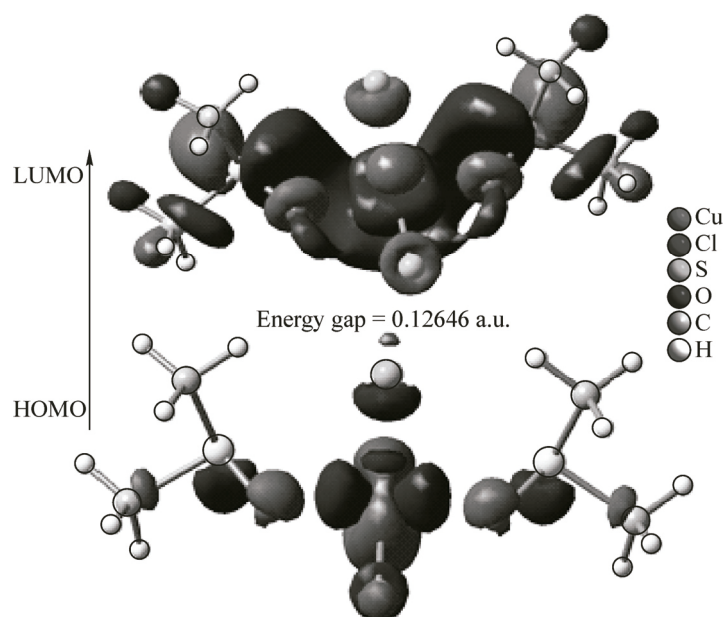
Fig. 5. Electron distribution of the HOMO and the LUMO energy levels of **I**

HOMO of the title compound presents a charge density localized mainly on both oxygen and chlorine atoms whereas LUMO is mostly on copper and sulfur atoms with a little charge density localized on carbon atoms. The gap energy ($E_{\text{LUMO}} - E_{\text{HOMO}}$) is 0.12646 a.u. We can see that this value is very low indicating a little energy barrier for a possible internal electronic transfer. HOMO and LUMO energies are given as $I = -E_{\text{HOMO}}$ and $A = -E_{\text{LUMO}}$, where A is the ionization potential and I is the electron affinity of the molecule. The energy gap between the HOMO and LUMO give the hardness. The global hardness was calculated by the expression $\eta = 1/2(E_{\text{LUMO}} - E_{\text{HOMO}})$. The electronic chemical potential, $\mu = 1/2(E_{\text{LUMO}} + E_{\text{HOMO}})$ and electrophilicity, $\omega = \mu^2/2\eta$ were also calculated and listed in Table 3. These have been defined [27, 28] and calculated using Koopman's theorem [29] for closed shell molecules.

CONCLUSIONS

The title compound dichlorobis(dimethylsulfoxide-O)copper(II) was synthesized and characterized by FT-IR, UV-visible, and single crystal X-ray diffraction. The complex crystallizes in the orthorhombic space group Pnma. The crystal structure consists of $CuCl_2(DMSO)_2$ moieties tied together by long Cu—Cl interactions to form infinite chains parallel to the [100] axis. The theoretical calculations were performed using the DFT method at the B3LYP/6-311G++(2d,2p) level. Also, the theoretical molecular structure was determined using DFT with the B3LYP hybrid functional in combination with the 6-31++G(2d,2p) basis set. The experimental geometrical parameters were in good agreement with those obtained by the theoretical calculation. The difference observed between the experimental

T a b l e 3

Calculated energy gaps and other molecular parameters of **I**

Molecular properties	Values, a.u.	Molecular properties	Values, a.u.
HOMO energy	–0.27011	Electron affinity (A)	0.14365
LUMO energy	–0.14365	Global hardness (η)	0.06323
Energy gap	0.12646	Chemical potential (μ)	–0.41376
Ionization potential (I)	0.27011	Global electrophilicity (ω)	1.35376

and computed values may be due to the fact that the computational study was performed for a single molecule in the gas phase, whereas the experimental values in the solid phase were recorded in the presence of intermolecular interactions. The MO energies and λ_{max} of the compound were also determined from the TD-DFT approach and the CPCM quantum model solvation in ethanol. The calculated HOMO and LUMO along with their plot have been presented for understanding the charge transfer occurring within the molecule.

REFERENCES

1. *Cotton F.A., Francis R.* // J. Am. Chem. soc. – 1960. – **82**. – P. 2986 – 2991.
2. *Cotton F.A., Francis R., Horrocks W.D.* // J. Phys. Chem. – 1960. – **64**. – P. 1534 – 1536.
3. *Cotton F.A., Francis R.* // J. Inorg. Nucl. Chem. – 1961. – **17**. – P. 62 – 68.
4. *Meek D.W., Straub D.K., Drago R.S.* // J. Am. Chem. Soc. – 1960. – **82**. – P. 6013 – 6016.
5. *Drago R.S., Meek D.W.* // J. Phys. Chem. – 1961. – **65**. – P. 1446.
6. *North A.C.T., Phillips D.C., Mathews F.S.* // Acta. Cryst. – 1968. – **A24**. – P. 351 – 359.
7. *Harms K., Wocadlo S.* XCAD4. University′ of Marburg, Germany, 1995.
8. *Farrugia L.J.* // J. Appl. Cryst. – 2012. – **45**. – P. 849 – 854.
9. *Sheldrick G.M.* SHELXS-97, SHELXL-97 // Acta Cryst. – 2008. – **A64**. – P. 112 – 122.
10. *Brandenburg K.* DIAMOND. Crystal Impact GbR, Bonn, Germany, 2001.
11. *Hohenberg P., Kohn W.* // Phys. Rev. – 1964. – **B136**. – P. 864.
12. *Kohn W.* // Phys. Rev. – 1964. – **133**. – P. 171 – 181.
13. *Becke A.* // J. Chem. Phys. – 1993. – **98**. – P. 5648 – 5652.
14. *Lee C., Yang W., Parr R.* // Phys. Rev. – 1988. – **B37**. – P. 785 – 789.
15. *Bauschlicher C.W., Partridge H.* // Chem. Phys. Lett. – 1995. – **240**. – P. 533 – 540.
16. *Frisch M.J. et al.* GAUSSIAN09. Revision A.01. Gaussian Inc., Wallingford, CT, USA, 2009.
17. *Dennington R.D., Keith T.A., Millam J.M.* GaussView 5.0.8, Gaussian Inc., 2008.
18. *Gokce H., Bahceli S.* // Spectrochim. Acta A Mol. Biomol. Spectrosc. – 2013. – **116**. – P. 242 – 250.
19. *Sundaraganesan N., Joshua B.D., Settu K.* // Spectrochim. Acta. A. Mol. Biomol. Spectrosc. – 2007. – **66**. – P. 381 – 388.
20. *Adams S.* softBV program, University of Göttingen, Germany (http: // kristall.unimki.dwdg.de/softBV/), 2003.
21. *Smith B.* Infrared Spectral, a Systematic Approach, CRC Press, Washington, DC, 1999.
22. *Gussoni M., Castiglioni C.O.* // J. Mol. Struct. – 2000. – **521**. – P. 1 – 8.
23. *Kalsi P.S.* Spectroscopy of Organic Compounds, New Age International (P) Limited, Publishers, 2009.
24. *Mohammed L.S., Hamza I.S., Muhi AL-Deen F.R., Muhyedeen B.R.J.* // J. Appl. Chem. – 2014. – **3**, N 5. – P. 2102 – 2121.
25. *Kosar B., Albayrak C.* // Spectrochim. Acta. – 2011. – **78A**. – P. 160 – 167.
26. *Powell B.J., Baruah T., Bernstein N., Brake K., McKenzie R.H., Meredith P., Pederson M.R.* // J. Chem. Phys. – 2004. – **12**. – P. 8608 – 8615.
27. *Parr R., Szentpaly L., Liu S.* // Am. Chem. Soc. – 1999. – **121**. – P. 1922 – 1924.
28. *Chattraj P., Maiti B., Sarkar U.* // J. Phys. Chem. – 2003. – **A107**. – P. 4973 – 4975.
29. *Koopmans T.A.* // Physica. – 1934. – **1**. – P. 104 – 113.